This article is published as part of the *Dalton Transactions* themed issue entitled:

Molecular Magnets

Guest Editor Euan Brechin
University of Edinburgh, UK
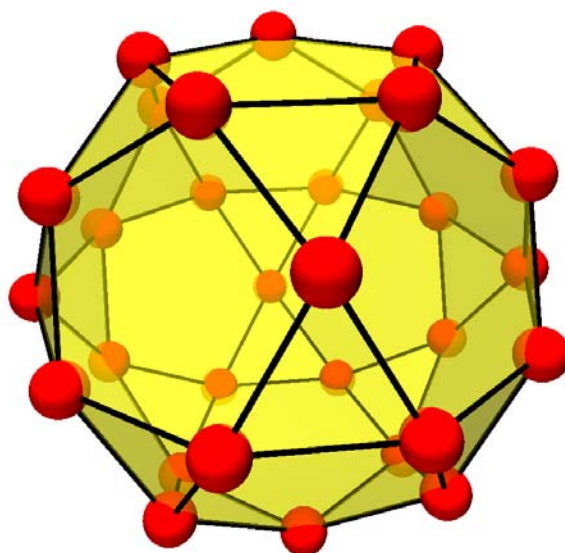
Published in issue 20, 2010 of *Dalton Transactions*

Image reproduced with permission of Jürgen Schnack

Articles in the issue include:

PERSPECTIVES:

Magnetic quantum tunneling: insights from simple molecule-based magnets
Stephen Hill, Saiti Datta, Junjie Liu, Ross Inglis, Constantinos J. Milios, Patrick L. Feng, John J. Henderson, Enrique del Barco, Euan K. Brechin and David N. Hendrickson, *Dalton Trans.,* 2010, DOI: 10.1039/c002750b

Effects of frustration on magnetic molecules: a survey from Olivier Kahn until today
Jürgen Schnack, *Dalton Trans.,* 2010, DOI: 10.1039/b925358k

COMMUNICATIONS:

Pressure effect on the three-dimensional charge-transfer ferromagnet [{Ru2(m-FPhCO2)4}2(BTDA-TCNQ)]
Natsuko Motokawa, Hitoshi Miyasaka and Masahiro Yamashita, *Dalton Trans.,* 2010, DOI: 10.1039/b925685g

Slow magnetic relaxation in a 3D network of cobalt(II) citrate cubanes
Kyle W. Galloway, Marc Schmidtmann, Javier Sanchez-Benitez, Konstantin V. Kamenev, Wolfgang Wernsdorfer and Mark Murrie, *Dalton Trans.,* 2010, DOI: 10.1039/b924803j

Visit the *Dalton Transactions* website for more cutting-edge inorganic and organometallic research
www.rsc.org/dalton

A family of double-bowl *pseudo* metallocalix[6]arene discs†

Seán T. Meally,[a] Cecelia McDonald,[a] Georgios Karotsis,[b] Giannis S. Papaefstathiou,[c] Euan K. Brechin,[b] Peter W. Dunne,[a] Patrick McArdle,[a] Nicholas P. Power[a] and Leigh F. Jones*[a]

We report the synthesis and magnetic characterisation of a series of planar [M_7] (M = Ni^{II}, Zn^{II}) disc complexes [Ni$_7$(OH)$_6$(L$_1$)$_6$](NO$_3$)$_2$ (**1**), [Ni$_7$(OH)$_6$(L$_1$)$_6$](NO$_3$)$_2$·2MeOH (**2**), [Ni$_7$(OH)$_6$(L$_1$)$_6$](NO$_3$)$_2$·3MeNO$_2$ (**3**), [Ni$_7$(OH)$_6$(L$_2$)$_6$](NO$_3$)$_2$·2MeCN (**4**), [Zn$_7$(OH)$_6$(L$_1$)$_6$](NO$_3$)$_2$·2MeOH·H$_2$O (**5**) and [Zn$_7$(OH)$_6$(L$_1$)$_6$](NO$_3$)$_2$·3MeNO$_2$ (**6**) (where HL$_1$ = 2-iminomethyl-6-methoxy-phenol, HL$_2$ = 2-iminomethyl-4-bromo-6-methoxy-phenol). Each member exhibits a double-bowl *pseudo* metallocalix[6]arene topology whereby the individual [M_7] units form molecular host cavities which are able to accommodate various guest molecules (MeCN, MeNO$_2$ and MeOH). Magnetic susceptibility measurements carried out on complexes **1** and **4** indicate weak exchange between the Ni^{II} centres.
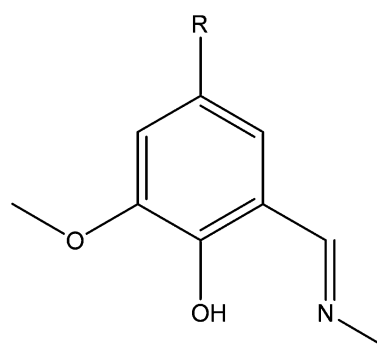
Introduction

Supramolecular chemistry has rapidly become a vast and multidisciplinary field with applications including catalysis,[1] anion sensing recognition,[2] gas sequestration/storage[3] and species transportation towards drug delivery,[4] and consequently is of interest to scientists of wide ranging disciplines. One particularly interesting facet of supramolecular chemistry concerns the expression of high degrees of local and extended topological control onto a molecule (*e.g.* a host unit) in terms of it partaking in intermolecular interactions with other species (*e.g.* a guest molecule). This is achieved *via* careful structural manipulation of these molecules (and molecular assemblies) giving rise to complex molecular architectures possessing targeted synergic chemical and physical properties. Although supramolecular host–guest chemistry has been readily exhibited and widely reported with a vast array of organic receptor moieties,[5] the engagement of magnetically interesting inorganic host units is still relatively rare.[6] The complementarity which has long existed between the fields of supramolecular chemistry and molecular magnetism has fascinated scientists for many years.[7] This was once again highlighted recently in the production of a tetranuclear [Mn$_4$] Single-Molecule magnet[8] and a [Mn$_4$Gd$_4$] magnetic cooler,[9] each built entirely using bowl-like calix[4]arene ligands - a cyclophane synonymous with host–guest supramolecular chemistry.[10] By employing this particular ligand the authors have purposefully exercised site specific cluster growth (*i.e.* the {Mn$_4$} and {Mn$_4$Gd$_4$} motifs can only be formed at the lower rim of the Calix[4]arene ligands) and spatial separation of the individual [Mn$_4$] units to promote magnetic dilution.

With this in mind we herein report the synthesis and characterization of a family of ferromagnetic planar disc [Ni$_7$] complexes which possess double-bowl metallocalix[6]arene topologies and themselves exhibit host–guest behaviour allowing direct comparison to supramolecular calix[*n*]arene behaviour. The work described in detail below serves as an extension to our initial findings, namely the report on the founder members of this extended family.[11]

Results and discussion

The first complex of this series to be discovered was the heptanuclear complex [Ni$_7$(OH)$_6$(L$_1$)$_6$](NO$_3$)$_2$ (**1**) which was obtained *via* the ethanolic reaction of Ni(NO$_3$)$_2$·6H$_2$O and HL$_1$ (Scheme 1) in the presence of NaOH. The green hexagonal crystals of **1** crystallize in the trigonal space group *P*-3*c*1 in approximately 30% yield (Fig. 1).‡ The core in **1** is best described as a body

[a]School of Chemistry, University Road, National University of Ireland, Galway, Ireland. E-mail: leigh.jones@nuigalway.ie; Tel: +353-091-49-3462
[b]School of Chemistry, Joseph Black Building, University of Edinburgh, West Mains Road, Edinburgh, Scotland, UK
[c]Laboratory of Inorganic Chemistry, Department of Chemistry, National and Kapodistrian University of Athens, Panepistimiopolis, Zografou 157 71, Greece

† Electronic supplementary information (ESI) available: Full experimental details on the synthesis of the ligands HL$_1$ and HL$_2$ available. CCDC reference numbers 758960–758962. For ESI and crystallographic data in CIF or other electronic format see DOI: 10.1039/b926704b

Scheme 1 Structure of the Schiff base ligands HL$_1$ and HL$_2$ utilised in this work (R = H (HL$_1$), Br (HL$_2$)).

‡ For crystal structure data for complexes **1**, **3** and **4** see CCDC 722288–722290 respectively.†

centred hexagon whereby six Ni^{II} ions surround a central Ni^{II} centre to form a planar disc. Although topologically analogous $[Mn_7]$,[12] $[Fe_7]$[13] and $[Co_7]$[14] complexes are known, the synthesis of **1** represents the first example for Ni^{II}. All Ni^{II} centres exhibit distorted octahedral geometries. The six μ_3-bridging OH^- ions (O1 and symmetry equivalent, s.e) link the central nickel (Ni1) to the six peripheral nickel ions (Ni2 and s.e.). The central Ni^{II} ion is located at a site with imposed $\bar{3}$ symmetry with the NO_3^- nitrogen atom (N2) sitting on a threefold axis. The remainder of the asymmetric unit comprises a second Ni^{II} centre (Ni2) along with one L^- unit and one hydroxy group (O1–H1) occupying general positions. Each of the six trigonal pyramidal OH^- ions are situated alternately above and below the $[Ni_7]$ plane (Fig. 1). The six singly deprotonated (at the phenolate site) L_1^- ligands bridge the peripheral Ni^{II} centres *via* a μ_2-η^1:η^2:η^1 coordination mode. These ligands are situated alternately above and below the $[Ni_7]$ plane which gives rise to a double-bowl conformation in which the $[Ni_7]$ core is the basal plane, reminiscent of a metallocalix[6]arene concave unit (Fig. 1). Full crystallographic parameters obtained for **1** (and all other members) are documented in Table 2.
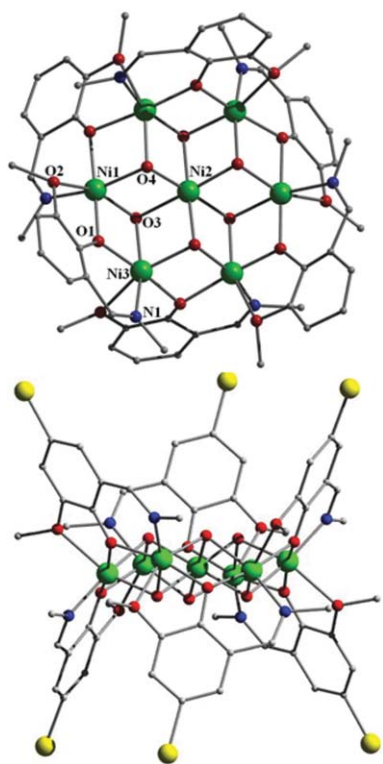
Fig. 1 Molecular structures of complexes **1** (top) and **4** (bottom) viewed perpendicular and parallel to the $[Ni_7]$ plane respectively. Colour code: Ni = green, O = red, N = blue, C = silver, Br = yellow.

Close scrutiny of the double-bowl conformation in **1** shows approximate bowl dimensions of 6.20 × 4.21 × 11.70 Å (base × depth × rim diameter). The $[Ni_7]$ units in **1** stack on top of one another resulting in the formation of pseudo-superimposable 1D columns whereby each moiety is spaced at a $[Ni_7]_{plane}$-$[Ni_7]_{plane}$ distance of 11.64 Å.[13] Furthermore the unit cell in **1** possesses four such 1D columns, each unit linked by a 120° rotation (Fig. SI3†). The $[Ni_7]$ moieties are connected into 1D columnar arrays *via* zig-zag shaped belts of NO_3^- anions (each comprising six NO_3^- ions),

located above and below the individual $[Ni_7]$ units with C–H⋯O bonding interactions between the NO_3^- oxygen atoms (one unique, O4) and protons (H1A and H5) of the L_1^- ligands (H1A⋯O4 = 2.59 Å and H5⋯O4 = 2.44 Å). The NO_3^- belts act as 'molecular zips' by pairing up individual $[Ni_7]$ complexes to form molecular cavities each of approximate volume ~265.9 Å³,[15] formed by two juxtaposed pseudo metallocalix[6]arene $[Ni_7]$ bowl units (Fig. 3). For complete molecular cavity dimensions in the crystal of **1** (and all other analogues) see Table 1.
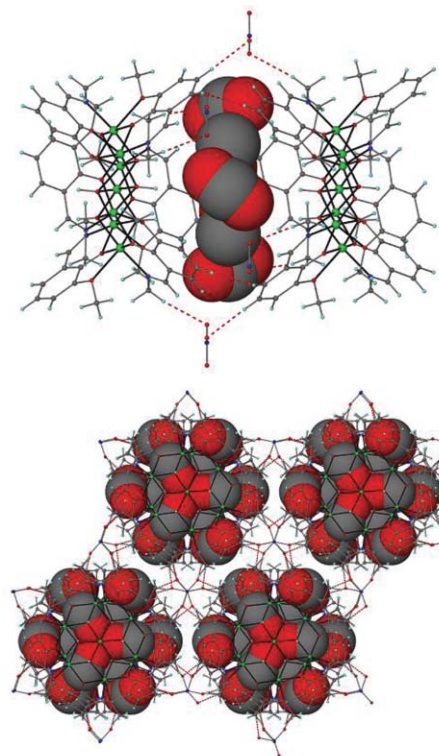
Fig. 2 (top) Crystal structure of **2** as viewed parallel to the $[Ni_7]$ cores; (bottom) Crystal packing observed in **2**. Dashed lines represent H-bonding interactions in between the individual $[Ni_7]$ units in **2** (*via* the NO_3^- anions). The guest disordered MeOH molecules are shown as space filled spheres (O = red, C = grey).

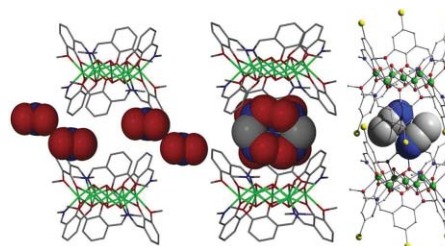**Fig. 3** Molecular structures of **1**, **3** and **4** highlighting (left): the empty cavity and belt of NO_3^- anions in **1**, (middle) the disordered guest $MeNO_2$ molecules in **3** and (right) the two MeCN guests located inside the cavities of **4**.

Although void of guest moieties, the fascinating double bowl metallocalix[6]arene cavities observed in **1** led to their investigation as rare examples of paramagnetic host receptors. Initial work involved the replacement of EtOH (used in production of the empty

Table 1 Molecular cavity dimensions observed in the crystals of **1–4**

	1	2	3	4
Cavity volume/Å³	265.9	293.7	283.8	155.9
Cavity dimensions/Å (base × depth × rim)	6.20 × 4.21 × 11.70	6.20 × 4.16 × 11.81	6.20 × 4.08 × 12.04	6.22 × 6.18 × 11.90
$[M_7]_{plane}$–$[M_7]_{plane}$ dist./Å	11.64	11.57	11.37	11.14

Table 2 Crystallographic data for complexes **1–4**

	1	2	3	4
Formula[a]	$C_{54}H_{66}N_8O_{24}Ni_7$	$C_{56}H_{66}N_8O_{26}Ni_7$	$C_{57}H_{75}N_{11}O_{30}Ni_7$	$C_{58}H_{66}Br_6N_{10}O_{24}Ni_7$
M_w	1622.12	1678.14	1709.25	2177.64
Crystal system	Trigonal	Trigonal	Trigonal	Monoclinic
Space group	P-3c1	P-3c1	P-3c1	$C2/c$
a/Å	13.806(2)	13.913(2)	13.933(2)	28.8575(14)
b/Å	13.806(2)	13.913(2)	13.933(2)	11.1352(3)
c/Å	23.270(5)	23.141(5)	22.742(5)	27.4079(13)
α (°)	90	90	90	90
β (°)	90	90	90	109.603(3)
γ (°)	120	120	120	90
V/Å³	3841.2(11)	3879.6(11)	3823.4(11)	8296.6(7)
Z	2	2	2	4
T/K	150	150	150	150
λ^b/Å	0.71070	0.71070	0.71070	0.71070
D^c/g cm⁻³	1.402	1.437	1.485	1.743
μ(Mo-Kα)/mm⁻¹	1.749	1.736	1.762	1.516
Meas./indep.(R_{int}) refl.	2306/1376 (0.0802)	2335/2034(0.0679)	2333/1835(0.0502)	7348/3779 (0.0511)
wR_2 (all data)	0.2446	0.2155	0.1725	0.1325
$R_1^{d,e}$	0.1209	0.0751	0.0604	0.1090
Goodness of fit on F^2	1.091	1.047	1.191	0.852

[a] Includes guest molecules. [b] Mo-Kα radiation, graphite monochromator. [c] w$R_2 = [\sum w(IF_o{}^2I − IF_c{}^2I)^2 / \sum wIF_o{}^2I^2]^{1/2}$. [d] For observed data. [e] $R_1 = \sum IIF_oI − IF_cII / \sum IF_oI$.

host (**1**)) with the smaller MeOH solvent in order to encourage guest occupancy. This proved successful with the isolation of the host–guest complex [Ni₇(OH)₆(L₁)₆](NO₃)₂·2MeOH (**2**), which crystallises in the same trigonal P-3c1 space group as **1** in ~40% yield. This improved yield, when compared to the preparation of **1**, is presumably due to the increased solubility of NaOH in MeOH. Complex **2** also exhibits a central Ni^{II} (Ni1) of imposed $\bar{3}$ symmetry and a N atom of the NO₃⁻ counter anion (N2) located on a threefold rotation axis. The molecular cavities in **2** are similar to those in **1** (6.20 × 4.16 × 11.81 Å (base × depth × rim diameter)), while the $[Ni_7]_{plane}$-$[Ni_7]_{plane}$ distance of 11.57 Å is also comparable to that of **1** (Table 1). Complex **2** differs with respect to **1** only in that the H-bonded cavities in **2** (of calculated volume of ~ 293.7 Å³) are of the required dimensions to accommodate two guest MeOH molecules. When small molecules are located within such highly symmetrical molecular cavities, it is common to observe crystallographic disorder and the MeOH guest molecules in **2** are no exception.

The first disordered MeOH guest (atoms C20–O10) has only 1/6th occupancy and thus periodically occupies positions in between the NO₃⁻ counter anions (which form the aforementioned zig-zag belt) and partakes in H-bonding interactions (O4···O10 = 2.86 Å). The second MeOH guest (C21–O9) lies within the molecular cavity in **2** at the midpoint between the two [Ni₇] planes (possessing a two-fold axis along the C–O vertex) where it is also disordered over three sites with respect to the three fold rotation axis inherent to the cell (Fig. 2). This central MeOH guest shows no

significant signs of supramolecular interactions within or outside its host cavity. This is not particularly surprising as this central MeOH guest moiety lies over 4 Å away from the nearest μ₃-OH⁻ protons (O1(H1)···O9 = 4.10 Å).

It was decided to attempt the encapsualtion of a larger guest molecule which would invoke H-bonding interactions within the molecular cavity and promote affinity towards its host receptor. It was decided to utilise MeNO₂ unit as a potential guest on the assumption that its O-atoms would interact with the H atoms of the μ₃-OH⁻ bridges within the [Ni₇] host cavity units. This was achieved, producing the complex [Ni₇(OH)₆(L₁)₆](NO₃)₂·3MeNO₂ (**3**), formed by dissolution and recrystallisation of **1** from MeNO₂ in ~15% yield.† In the crystals of **3** (Fig. 4) the host cavity has a calculated volume of 283.8 Å³ and is occupied by three MeNO₂ guests which are related crystallographically *via* a three fold rotation. As observed in **2**, the trigonal planar MeNO₂ guests also experience disorder whereby the methyl carbon atoms (C10 and s.e) lie on a two fold axis. These orientations are most likely to exist in the up-down-up antiparallel configuration with respect to the three fold rotation symmetry they share, as any other spatial arrangement would result in significant steric effects (Fig. 3). As predicted the three interact within the cavity *via* hydrogen bonding interactions between their O-atoms (O5 and O6) and the nearby μ₃-OH⁻ protons of the two [Ni₇] units which line the cavity floors (O1···O5 = 3.08 Å; O1···O6 = 3.25 Å).

In order to alter the interior size and shape of the molecular cavities highlighted in **1–3** towards subsequent modification
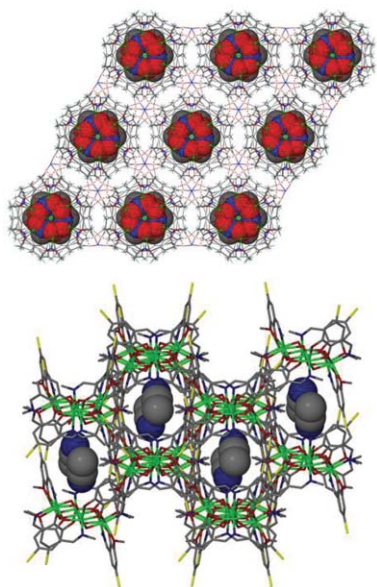
Fig. 4 Crystal packing observed in the crystals of **3** (top) and **4** (bottom) showing the molecular cavities accommodating guest $MeNO_2$ (red spheres), and MeCN (grey/blue spheres) solvent molecules respectively. NO_3^- counter anions have been omitted for clarity in figure depicting complex **4**.

and/or control of guest preference, it was decided to attempt to increase the bowl depth (in relation to complexes **1–3**) by utilising the Br-analogue of HL_1, namely the pro-ligand 2-iminomethyl-4-bromo-6-methoxy-phenol (HL_2). To this end an ethanolic solution of $Ni(NO_3)_2 \cdot 6H_2O$, the ligand HL_2 and NaOH was left to stir for 4 h. The mother liquor was then left to evaporate slowly, but no crystalline product was obtained. The subsequent green powder produced was redissolved in numerous potential guest solvents ($MeOH$, $MeNO_2$, MeCN). Interestingly only the MeCN guest species was successfully incorporated in the form of the complex $[Ni_7(OH)_6(L_2)_6](NO_3)_2 \cdot 2MeCN$ (**4**), which was formed in ~23% yield and crystallises in the monoclinic $C2/c$ space group (*cf.* **1–3**).† In this case each cavity accommodates two MeCN molecules which exhibit a head-to-tail conformation (Fig. 3 (right)). The MeCN guests are held in place *via* H-bonding between their N-atoms (N5) and a proton (H3A) of an μ_3-OH^- bridging ion belonging to the neighbouring $[Ni_7(OH)_6]$ core (N5···H3A(O3) = 2.36 Å).

The central Ni^{II} ion (Ni4) located at the centre of **4** lies on an inversion centre with the remaining three metal centres (Ni1-3) and all other atoms in the asymmetric unit occupying general positions. The employment of L_2^- in the construction of **4** does indeed significantly alter the cavity size and shape, as the crystal structure shows the formation of a deeper bowl of dimesions $6.22 \times 6.18 \times 11.90$ Å (base × depth × rim diameter). As observed in **1–3** the individual $[Ni_7]$ units in **4** again arrange into superimposable 1D columns, which propagate along the *b* direction of the unit cell. The stacking of the $[Ni_7]$ units along *b* is supported by two complementary O–H···Br interactions which involve one μ_3-OH^- (H1) of a $[Ni_7]$ unit and the bromine atom (Br1) of a neighbouring $[Ni_7]$ moiety (H1···Br1 = 2.82 Å). These hydrogen bonds direct molecular cavities which differ from those in **1–3** as here they are tilted with respect to the $[Ni_7]$ planes and are interlocked in

a staggered arrangement (Fig. 3). The $[Ni_7]_{plane}$-$[Ni_7]_{plane}$ distance inside the cavity is 11.14 Å and represents a cavity height reduction of ~0.4 Å *cf.* **1–3**. We postulate that this is attributed to the significant H-bonding affinity of the pendant Br-atoms (Br1) in **4**, producing a more tightly embraced cavity of approximate volume 155.9 Å³, which is significantly smaller than those of **1** (265.9 Å³), **2** (293.7 Å³) and **3** (283.8 Å³). For full details on the individual H-bonding parameters in complexes **1–6** see table SI2.†

Efforts to encapsulate MeCN and $MeNO_2$ solvent guests inside the cavities of **2** and **4**, respectively, were unsuccessful. These findings suggest that guest molecules can only be placed within such cavities if and when they are able to orientate themselves into certain topologies comprising symmetry elements compatible with their host lattices. This hypothesis is supported by the formation of complex **3** in which three MeOH guests, linked *via* a three-fold rotation axis, are accommodated inside the trigonal P-3c1 cell whereas attempts at producing a MeOH guest analogue to **4** (in a monoclinic $C2/c$ cell) remain fruitless. It must be noted that the size and shape of the molecular cavities in such complexes will also reflect their resultant guests and must also be considered here. Attempts at encapsulating larger organic moieties (inc. fluorophores, amino acids and anions) have so far been unsuccessful. Indeed all attempts at such encapsulation simply resulted in the recrystallisation of complexes **1–4** (depending on the synthon employed). We may postulate that this is due to the ubiquitous nature of the solvent molecules present in our reaction mixtures which will inevitably become guests within our host $[Ni_7]$ discs.

3D connectivity of 1–4

Complexes **1–3** crystallise in the trigonal P-3c1 space group and only differ in terms of their guest occupancy and therefore are analogous in terms of their 3D connectivity. The $[Ni_7]$ columns in their unit cells are connected *via* H-bonds to adjacent 1D $[Ni_7]$ columns. These connections are manifested by a myriad of H-bonding interactions between the NO_3^- counter anions and the individual $[Ni_7]$ moieties. More specifically each $[Ni_7]$ is H-bonded to twelve NO_3^- counter anions which in turn connect to six other $[Ni_7]$ units thus creating a (6,12)-connected net with a $(4^{15})_2(4^{48}.6^{18})$-**alb** topology (Fig. 5).[16,17] As previously stated, $[Ni_7(OH)_6(L_2)_6](NO_3)_2 \cdot 2MeCN$ (**4**) crystallises in the monoclinic $C2/c$ space group and as such possesses a 3-D connectivity different to that of **1–3**. The 1D columnar stacks of $[Ni_7]$ units in **4** are linked by C–H···Br interactions through the Br atoms (Br2 and Br3) of the bridging L_2^- ligands and the –CH_3 protons (H18B and H27B) of adjacent $[Ni_7]$ moieties (H18B···Br3 = 2.93 Å, H27B···Br2 = 2.70 Å and *s.e*). The result is a 3-D connectivity comprising a 10-connected net with a $(3^{12}.4^{28}.5^5)$-**bct** topology (Fig. 5).[16,17]

IR spectroscopic studies on the host complexes **2**, **3** and **4** were performed to ascertain whether their guest molecules remained within their respective H-bonded cavities on drying. CHN analysis on samples of complexes **2–4** were consistent with guest residency. The IR spectrum of $[Ni_7(OH)_6(L_1)_6](NO_3)_2 \cdot 2MeOH$ (**2**) showed broad OH stretching bands (centred at 3416 cm⁻¹) attributable to both the μ_3-OH^- bridges and MeOH guest solvent molecules. However there was also a possibility that such bands were due to adsorbed MeOH solvent molecules and therefore the same
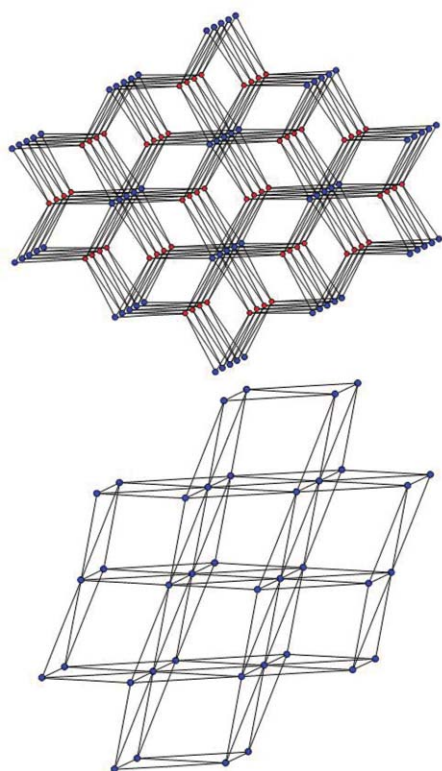
Fig. 5 (top) The (6,12)-connected net with a $(4^{15})_2(4^{48}.6^{18})$-**alb** topology in **1–3**. Large blue spheres represent the 12-connected [Ni$_7$] units. Smaller red spheres represent the 6-connected NO$_3^-$. (bottom) The 10-connected $(3^{12}.4^{28}.5^5)$-**bct** in **4** where the blue spheres represent the 10-connected [Ni$_7$] units.

sample was subsequently dried under vacuum for 2 h prior to re-analysis of its IR spectrum. It was found that the initial broad OH stretching band had lost intensity on drying and was now centred at 3406 cm^{-1} (Fig. SI4†). Subsequent elemental analysis on this same sample analysed as the empty [Ni$_7$(OH)$_6$(L$_1$)$_6$](NO$_3$)$_2$ (**2**) complex. Similarly the IR spectrum of **3** gave peaks at 1337 and 1555 cm^{-1} which are characteristic for the asymmetric and symmetric NO stretching of the guest MeNO$_2$ molecules respectively. Subsequent vacuum drying of **3** (for 2 h) resulted in the loss of these vibrational resonances indicating egress of the MeNO$_2$ guests which was also subsequently confirmed by elemental analysis. The facile removal of the MeOH and MeNO$_2$ guests in **2** and **3** respectively is consistent with their crystal structures and more specifically in the way that their host cavities are held only *via* weak hydrogen bonding interactions and by no means form tightly bound enclosures. The IR spectrum of [Ni$_7$(OH)$_6$(L$_2$)$_6$](NO$_3$)$_2$·2MeCN (**4**) exhibits a weak resonance at 2256 cm^{-1} corresponding to a CN stretch indicative of the enclosed MeCN guest molecules. Interestingly and unlike complexes **2** and **3** this peak at 2256 cm^{-1} is not lost upon substantial vacuum drying (Fig. SI5†), while no significant change is seen in its subsequent CHN microanalysis. This observation suggests the MeCN guests cannot readily exit the host cavities in **4** which may be attributed to its distinct (*cf.* **1–3**) and more tightly locked double-bowl enclosures formed *via* the H-bonding pendant Br-groups (*vide infra*).

In order to further probe potential affinities of our guest solvent molecules for their [Ni$_7$] hosts using NMR techniques the diamagnetic [Zn$_7$] analogues [Zn$_7$(OH)$_6$(L$_1$)$_6$](NO$_3$)$_2$·2MeOH·H$_2$O (**5**) (Fig. SI6†) and [Zn$_7$(OH)$_6$(L$_1$)$_6$](NO$_3$)$_2$·3MeNO$_2$ (**6**) (Fig. 6) were synthesized (for crystallographic information see ESI). The structure of [Zn$_7$(OH)$_6$(L$_1$)$_6$](NO$_3$)$_2$·3MeNO$_2$ (**6**) is analogous to that of its Ni^{II} analogue (complex **3**) with a slightly larger cavity volume of 295.4 Å^3; however the connectivity in [Zn$_7$(OH)$_6$(L$_1$)$_6$](NO$_3$)$_2$·2MeOH·H$_2$O (**5**) differs slightly to that of its counter part [Ni$_7$(OH)$_6$(L$_1$)$_6$](NO$_3$)$_2$·2MeOH (**2**). The [Zn$_7$] units in (**5**) are held in 2D layers running parallel to the *ab* plane *via* the NO$_3^-$ anions, which sit above and below the individual heptanuclear complexes with C–H···O bonding interactions between the NO$_3^-$ oxygen atoms (one unique, O4) and protons (one unique, H5) of the L$_1^-$ ligands (H5···O4 = 2.46 Å). In this arrangement, each [Zn$_7$] is H-bonded to six NO$_3^-$ anions with the latter being connected to three [Zn$_7$] units thus creating a (3,6) layer. Although the NO$_3^-$ ions do not hold the [Zn$_7$] moieties of neighbouring layers, the (3,6) layers stack with the [Zn$_7$] forming columnar arrays like those found in complexes **1**, **2**, **3** and **5**, giving rise to molecular cavites (each of approximate volume ~ 280.4 Å^3 with a [Zn$_7$]$_{plane}$-[Zn$_7$]$_{plane}$ distance of 11.68 Å), formed by two juxtaposed pseudo metallocalix[6]arene [Zn$_7$] bowl units. Those cavities are of the required size and shape to accommodate two guest MeOH and one H$_2$O solvent molecules. These are related crystallographically *via* a three fold rotation.
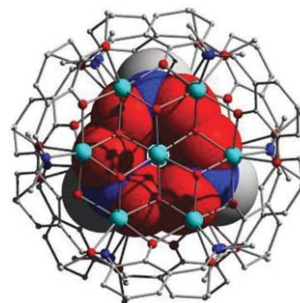

Fig. 6 Crystal structure of **6** as viewed along a 1D column of [Zn$_7$] units. Large space-fill spheres represent the three guest MeNO$_2$ moieties.

By direct crystallographic comparison it becomes clear that the cavities of **1** (265.9 Å^3), **2** (293.7 Å^3), **3** (283.8 Å^3), **5** (280.4 Å^3) and **6** (295.4 Å^3) are very similar. The rather small differences are due to the slightly different orientations of the [M$_7$] molecules in the crystals. From this we may draw the conclusion that the guests and/or the H-bonding with the NO$_3^-$ do not play an important role in the resultant cavity size.

Solution studies

Despite the rather poor solubility of this class of compound UV-vis studies on MeOH and MeCN solutions of [Ni$_7$(OH)$_6$(L$_1$)$_6$](NO$_3$)$_2$·2MeOH (**2**) were successfully performed (Fig. SI7†). Both solutions showed similar absorptions at approximately 230, 270 and 356 nm. A fourth sharp transition in the methanolic solution of **2** is observed at 205 nm which has been cut off in the analogous MeCN solution spectrum. The transitions at ~205, 230 and 270 nm are as a result of $\pi \rightarrow \pi^*$ excitations (ε values ranging from 42.8–110.2 × 10^3 dm^3 mol^{-1} cm^{-1}), while

the absorptions at 356 nm correspond to the $n \rightarrow \pi^*$ excitations occurring in both solutions of **2**. No absorptions indicative of d-d transitions are observed and if present are presumably masked by the presence of L_1^- in **2**. This assumption is supported by the UV-vis spectra of MeOH and MeCN solutions of the Zn^{II} sibling $[Zn_7(OH)_6(L_1)_6](NO_3)_2 \cdot 2MeOH \cdot H_2O$ (**5**), whose absorptions are analogous to those observed in **2** (Fig. SI8†) with no possibility of any significant d-d transitions. Furthermore the UV-vis spectra obtained from MeOH and MeCN solution of HL_1 and HL_2 (Fig. SI1 and SI2 respectively†) showed similar absorptions to those of $[Ni_7]$ (**2**) and $[Zn_7]$ (**5**), although on comparison appearing less defined presumably due to their more symmetric nature when incorporated into the $[M_7]$ complex.

Magnetic susceptibility studies

Magnetic susceptibility measurements were obtained on crystalline samples of $[Ni_7(OH)_6(L_1)_6](NO_3)_2$ (**1**) and $[Ni_7(OH)_6(L_2)_6](NO_3)_2 \cdot 2MeCN$ (**4**) in the 300–5 K temperature range (Fig. 7). The room temperature $\chi_m T$ values of 7.76 and 7.90 cm^3 mol^{-1} K respectively are slightly larger than the value expected for seven non interacting Ni^{II} ions (~ 7.7 cm^3 mol^{-1} K assuming $g = \sim 2.1$). As the temperature is decreased the values of $\chi_m T$ increase slowly, reaching maximum values of ~8.5 cm^3 K mol^{-1} at 40 K for **1** and ~10 cm^3 K mol^{-1} at 25 K for **4**, before decreasing below these temperatures to minimum values at 5 K of ~5.5 cm^3 K mol^{-1} (**1**) and ~7.9 cm^3 K mol^{-1} (**4**). This behaviour is suggestive of very weak ferromagnetic intra-molecular exchange between the Ni^{II} ions in both complexes, with their low temperature ($T < 40$ K) decreases in $\chi_m T$ ascribed to relatively strong inter-molecular antiferromagnetic exchange, consistent with the extensive H-bonding observed in the crystals of **1** and **4**. The maxima in $\chi_m T$ for **1** and **4** are well below that expected for an isolated $S = 7$ spin ground state which would give a $\chi_m T$ value of approximately 31 cm^3 K mol^{-1} (assuming $g = 2.10$). Fitting of the $1/\chi_m$ versus T data to the Curie–Weiss law using only the 300–50 K data affords Weiss constants (Θ) of +18.7 K (**1**) and +29.0 K (**4**) (Fig. SI9†), suggestive of weak ferromagnetic exchange. Several factors proclude the fitting or simulation of the susceptibility data: a) the presence of numerous different exchange interactions; b) the presence of relatively strong intermolecular interactions; c) the weak exchange between the metal centres and the likelihood that J will be comparable to the single ion zfs (weak exchange limit) and thus the presence of multiple low lying states that cannot properly be described as total S states. This scenario is supported by the magnetisation versus field data carried out in the 2–7 K temperature and 0.5–7.0 T magnetic field ranges (Fig. 7 (inset) (**1**) and Fig. SI10 (**4**)†). For an isolated spin ground state one would expect a rapid initial increase in M, with saturation of the magnetisation achieved for relatively low fields. However for both **1** and **4** M increases only slowly with H, indicative of the population of low lying levels with smaller magnetic moment, which only become depopulated with the application of larger fields. Our ability to make the analogous Zn^{II} complexes will therefore prove important for future studies. Doping experiments in which we make highly diluted $[Ni_7]$ clusters in $[Zn_7]$ matrices and study their behaviour by both SQUID magnetometry and EPR spectroscopy are currently in progress and will be reported at a later date.
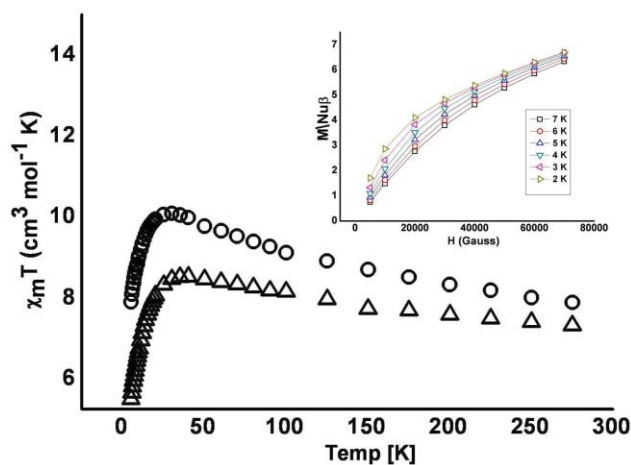

Fig. 7 Plot of $\chi_m T$ vs. T for complexes **1**($\triangle$) and **4** ($\bigcirc$) in the 300–5 K temperature range (measured in an applied field of 0.1 T). (Inset) Plot of $M/N\mu\beta$ vs. H (G) carried out on complexes **1** in the 2–7 K temperature range and 0.5–7 T magnetic field range.

Conclusions

We have reported the syntheses, structures and solid and solution state characterisation of a family of $[Ni_7]$ and $[Zn_7]$ planar hexagonal disc complexes. This family may also be described as *pseudo* metallocalix[6]arene complexes due to their double-bowl topologies which have shown to act as host cavities accommodating numerous guest solvent molecules. The magnetic behaviour of the Ni^{II} discs is complicated by the presence of relatively strong intermolecular interactions and weak intramolecular exchange and thus the isolation of the diamagnetic Zn^{II} analogues and the examination of the diluted $[Ni_7]$ discs promises to afford much useful information. Further progress of the work will include the functionalisation of the ligands HL_1 and HL_2 at their upper rim positions (R group in Scheme 1) in order to a) preferentially attract specific guest species and b) increase their solubility towards future ^1H NMR host–guest titration studies. Solid state NMR studies will also be investigated.

Experimental

Infra-red spectra were recorded on a Perkin Elmer FT-IR *Spectrum One* spectrometer equipped with a Universal ATR Sampling accessory (NUI Galway). UV-visible studies were carried out on a Cary *100 Scan* (Varian) spectrophotometer. Elemental analysis was carried at the School of Chemistry microanalysis service at NUI Galway. Variable-temperature, solid-state direct current (dc) magnetic susceptibility data down to 1.8 K were collected on a Quantum Design MPMS-XL SQUID magnetometer equipped with a 7 T dc magnet. Diamagnetic corrections were applied to the observed paramagnetic susceptibilities using Pascal's constants.

Syntheses

All reactions were performed under aerobic conditions and all reagents and solvents were used as purchased.

Synthesis of $[Ni_7(OH)_6(L_1)_6](NO_3)_2$ (1). Ni(NO$_3$)$_2 \cdot 6H_2O$ (0.25 g, 0.85 mmol), HL_1 (0.14 g, 0.85 mmol) and NaOH (0.034 g, 0.85 mmol) were dissolved in 30 cm^3 EtOH and stirred for 4 h.

The resultant green solution was then filtered and allowed to stand. X-Ray quality crystals of **1** were obtained in 30% yield upon slow evaporation. Elemental analysis calculated (%) for $C_{54}H_{66}N_8O_{24}Ni_7$ (**1**): C, 39.98; H, 4.10; N, 6.91; Found: C, 39.76; H, 4.18; N, 6.85. FT-IR (cm^{-1}): 3415 (w), 2968 (w), 2932 (w), 1627 (s), 1602 (w), 1559 (w), 1459 (m), 1406 (w), 1315 (s), 1221 (s), 1171 (w), 1148 (w), 1072 (m), 1044 (w), 1018 (w), 963 (m), 864 (m), 828 (w), 793 (m), 743 (s).

[Ni$_7$(OH)$_6$(L$_1$)$_6$](NO$_3$)$_2$·2MeOH (2). Ni(NO$_3$)$_2$·6H$_2$O (0.25 g, 0.86 mmol), HL$_1$ (0.145 g, 0.86 mmol) and NaOH (0.04 g, 1.00 mmol) were dissolved in 30 cm^3 MeOH and stirred for 3 h. The resultant green solution was then filtered and allowed to stand. X-Ray quality hexagonal crystals of **2** were obtained in 40% yield upon slow evaporation of the mother liquor. Elemental analysis on 'wet' sample of **2** calculated (%) for $C_{56}H_{74}N_8O_{26}Ni_7$ (**2**·2MeOH): C, 39.95; H, 4.10; N, 6.90; Found: C, 40.21; H, 4.43; N, 7.15. Elemental analysis on vacuum dried sample of **2** calculated (%) as $C_{54}H_{66}N_8O_{24}Ni_7$ (**2**): C, 39.99; H, 4.10; N, 6.91; Found: C, 39.69; H, 4.37; N, 7.03. FT-IR (cm^{-1}): 3402 (b), 2932 (w), 2817 (w), 1627 (s), 1603 (w), 1561 (w), 1459 (m), 1436 (m), 1407 (w), 1338 (m), 1314 (s), 1240 (w), 1222 (s), 1169 (w), 1147 (w), 1073 (m), 1042 (w), 1018 (w), 965 (m), 864 (m), 828 (w), 789 (m), 741 (s). UV/vis (MeOH): λ_{max} [nm] (ε_{max} 10^3 dm^3 mol^{-1} cm^{-1}): 205 (84.6), 231 (108.5), 268 (46.3), 356 (21.4). (MeCN): λ_{max} [nm] (ε_{max} 10^3 dm^3 mol^{-1} cm^{-1}): 230 (110.2), 268 (42.8), 356 (15.8).

[Ni$_7$(OH)$_6$(L$_2$)$_6$](NO$_3$)$_2$·3MeNO$_2$ (3). The reaction mixture obtained from **1** was filtered and the filtrate left to evaporate to dryness. The resultant green solid was then redissolved in 10 cm^3 MeNO$_2$ whereby green hexagonal crystals of **3** were obtained in 10% yield upon slow Et$_2$O diffusion. Elemental analysis calculated (%) for $C_{57}H_{75}N_{11}O_{30}Ni_7$ (**3**·3MeNO$_2$): C, 37.93; H, 4.19; N, 8.54; Found: C, 38.31; H, 4.59; N, 8.29. FT-IR (cm^{-1}): 3625 (w), 2931 (w), 1628 (s), 1601 (m), 1555 (s), 1476 (s), 1460 (s), 1433 (m), 1407 (m), 1337 (m), 1316 (m), 1221 (m), 1171 (w), 1147 (w), 1086 (w), 1072 (w), 1018 (w), 865 (w), 795 (w), 743 (w).

[Ni$_7$(OH)$_6$(L$_2$)$_6$](NO$_3$)$_2$·2MeCN (4). Ni(NO$_3$)$_2$·6H$_2$O (0.25 g, 0.85 mmol), HL$_2$ (0.21 g, 0.85 mmol) and NaOH (0.034 g, 0.85 mmol) were dissolved in 30 cm^3 EtOH and stirred for 4 h. The resultant green precipitous solution was then filtered and evaporated to dryness. The green solid was then redissolved in MeCN and from which crystals of **4** were obtained upon Et$_2$O diffusion in 23% yield. Elemental analysis calculated (%) for $C_{58}H_{66}N_{10}O_{24}Br_6Ni_7$ (**4**·2MeCN): C, 31.99; H, 3.06; N, 6.43; Found: C, 31.77; H, 3.28; N, 6.56. FT-IR (cm^{-1}): 3620 (w), 3261 (wb), 2927 (w), 2256 (w), 1629 (s), 1592 (w), 1543 (w), 1457 (m), 1457 (m), 1393 (m), 1352 (m), 1306 (s), 1236 (m), 1212 (m), 1150 (w), 1093 (w), 1040 (w), 1018 (w), 968 (w), 956 (w), 857 (w), 842 (w), 827 (w), 790 (w), 754 (w), 713 (w), 690 (w).

[Zn$_7$(OH)$_6$(L$_1$)$_6$](NO$_3$)$_2$·2MeOH·1H$_2$O (5). Zn(NO$_3$)$_2$·6H$_2$O (0.25 g, 0.85 mmol), HL$_1$ (0.14 g, 0.85 mmol) and NaOH (0.034 g, 0.85 mmol) were dissolved in 30 cm^3 MeOH and stirred for 2 h. The resultant yellow solution was then filtered and X-ray quality crystals of **5** were obtained in 35% yield upon slow evaporation. Elemental analysis calculated (%) for $C_{56}H_{74}N_8O_{26}Zn_7$ (**5**): C, 38.81; H, 4.30; N, 6.47; Found: C, 38.87; H, 4.65; N, 6.61. FT-IR (cm^{-1}): 3406 (b), 2931 (w), 2823 (w), 1636 (s), 1602 (w), 1561 (w), 1459 (m), 1408 (w), 1368 (m), 1330 (m), 1308 (s), 1221 (s), 1173 (w), 1148 (w), 1093 (m), 1077 (w), 1013 (w), 967 (m), 860 (m), 828 (w), 793 (m), 743 (s). UV/vis (MeOH): λ_{max} [nm] (ε_{max} 10^3 dm^3 mol^{-1} cm^{-1}): 202 (108.3), 226.9 (146.4), 267 (71.1), 350 (27.9). (MeCN): λ_{max} [nm] (ε_{max} 10^3 dm^3 mol^{-1} cm^{-1}): 227 (242.6), 267 (103.6), 350 (44.0).

[Zn$_7$(OH)$_6$(L$_1$)$_6$](NO$_3$)$_2$·3MeNO$_2$ (6). Zn(NO$_3$)$_2$·6H$_2$O (0.25 g, 0.85 mmol), HL$_1$ (0.14 g, 0.85 mmol) and NaOH (0.034 g, 0.85 mmol) were dissolved in 30 cm^3 EtOH and stirred for 3 h. The resultant yellow solution was then filtered and evaporated to dryness. The resultant solid was then redissolved in MeNO$_2$ from which X-ray quality crystals of **6** were obtained in ~ 10% yield. Elemental analysis calculated (%) for $C_{57}H_{75}N_{11}O_{30}Zn_7$ (**6**): C, 36.97; H, 4.08; N, 8.32; Found: C, 37.02; H, 4.17; N, 8.44. FT-IR (cm^{-1}): 3418 (w), 2967 (w), 2930 (w), 1625 (s), 1601 (w), 1561 (w), 1459 (m), 1405 (w), 1319 (s), 1220 (s), 1168 (w), 1149 (w), 1072 (m), 1041 (w), 1016 (w), 960 (m), 860 (m), 829 (w), 789 (m), 743 (s).

Acknowledgements

References

1 J. O. Magrans, A. R. Ortiz, M. A. Molins, P. H. P. Lebouille, J. Sanchez-Quesada, P. Prados, M. Pons, F. Gago and J. de Mendoza, *Angew. Chem., Int. Ed. Engl.*, 1996, **35**, 1712.
2 (*a*) J. L. Atwood, K. T. Holman and J. W. Steed, *Chem. Commun.*, 1996, 1401–1407; (*b*) P. D. Beer, *Chem. Commun.*, 1996, 689–696; (*c*) P. A. Gale, J. L. Sessler and V. Krail, *Chem. Commun.*, 1998, 1–8.
3 S. J. Dalgarno, P. K. Thallapally, L. J. Barbour and J. L. Atwood, *Chem. Soc. Rev.*, 2007, **36**, 236.
4 (*a*) W. Yang and M. M. De Villiers, *Eur. J. Pharm. Biopharm.*, 2004, **58**, 629; (*b*) W. Yang and M. M. De Villiers, *J. Pharm. Pharmacol.*, 2004, **56**, 703–708; (*c*) W. Yang and M. M. De Villiers, *AAPS J.*, 2005, **7**, E241–E248.
5 For examples see: (*a*) T. Heinz, D. M. Rudkevich and J. Rebek Jr., *Nature*, 1998, **394**, 764–766; (*b*) M. D. Pluth and K. N. Raymond, *Chem. Soc. Rev.*, 2007, **36**, 161–171 and references herein; (*c*) P. Restorp, O. B. Berryman, A. C. Sather, D. Ajami and J. Rebek Jr., *Chem. Commun.*, 2009, 5692–5694.
6 (*a*) O. D. Fox, N. K. Dalley and R. G. Harrison, *Inorg. Chem.*, 1999, **38**, 5860–5863; (*b*) R. G. Harrison, J. L. Burrows and L. D. Hansen, *Chem.–Eur. J.*, 2005, **11**, 5881–5888; (*c*) E. Pardo, K. Bernot, F. Lloret, M. Julve, R. Ruiz-Garcia, J. Pasan, C. Ruiz-Perez, D. Cangusso, V. Costa, R. Lescouezec and Y. Journaux, *Eur. J. Inorg. Chem.*, 2007, 4569–4575; (*d*) O. D. Fox, J. Cookson, E. J. B. Wilkinson, M. G. B. Drew, E. J. MacLean, S. J. Teat and P. D. Beer, *J. Am. Chem. Soc.*, 2006, **128**, 6990–7002; (*e*) I. Imaz, J. Hemando, D. Ruiz-Molina and D. Maspoch, *Angew. Chem., Int. Ed.*, 2009, **48**, 2245–2329; (*f*) M. Yoshizawa, J. K. Klosterman and M. Fujita, *Angew. Chem., Int. Ed.*, 2009, **48**, 3418–3438 and references herein.
7 O. Kahn, *Magnetism*: *A Supramolecular Function* (NATO Science Series) and references herein.
8 G. Karotsis, S. J. Teat, W. Wernsdorfer, S. Piligkos, S. J. Dalgarno and E. K. Brechin, *Angew. Chem., Int. Ed.*, 2009, **48**, 8285–8288.
9 G. Karotsis, M. Evangelisti, S. J. Dalgarno and E. K. Brechin, *Angew. Chem., Int. Ed.*, 2009, **48**, 9928–9931.
10 J. W. Steed and J. L. Atwood, *Supramolecular Chemistry* (Wiley). 2000.
11 S. T. Meally, G. Karotsis, E. K. Brechin, G. S. Papaefstathiou, P. W. Dunne, P. McArdle and L. F. Jones, *CrystEngComm*, 2010, **12**, 59, DOI: 10.1039/b914538a.
12 (*a*) T. C. Stamatatos, K. M. Poole, D. Fouget-Alblol, K. A. Abboud, T. A. O'Brien and G. Christou, *Inorg. Chem.*, 2008, **47**, 6593; (*b*) N. C.

Harden, M. A. Bolcar, W. Wernsdorfer, K. A. Abboud, W. E. Streib and G. Christou, *Inorg. Chem.*, 2003, **42**, 7067; (*c*) M. A. Bolcar, S. M. J. Aubin, K. Folting, D. N. Hendrickson and G. Christou, *Chem. Commun.*, 1997, 1485; (*d*) B. Pilawa, M. T. Kelemen, S. Wanka, A. Geisselmann and A. L. Barra, *Europhys. Lett.*, 1998, **43**, 7; (*e*) T. C. Stamatatos, K. M. Poole, D. Foguet-Albiol, K. A. Abboud, T. E. O'Brien and G. Christou, *Inorg. Chem.*, 2008, **47**, 6593.

13 H. Oshio, N. Hoshino, T. Ito, M. Nakano, F. Renz and H. Gütlich, *Angew. Chem., Int. Ed.*, 2003, **42**, 223.

14 S.-H. Zhang, Y. Song, H. Liang and M.-H. Zeng, *CrystEngComm*, 2009, **11**, 865.

15 L. J. Barbour, *MCAVITY: Program for calculating the molecular volume of closed capsules*, University of Missouri-Columbia, Columbia, MO, USA, 2003, http://www.x-seed.net/cavity.html. The free volume within the cavities of **1-4** was calculated in the absence of guests.

16 V. A. Blatov, *IUCr CompComm Newsletter*, 2006, 4–38.

17 M. O'Keeffe, M. A. Peskov, S. J. Ramsden and O. M. Yaghi, *Acc. Chem. Res.*, 2008, **41**, 1782.